

Intelligent Speed Controller Design for a Spark Ignition Engine

Dr. Saleh Ismael Nejem
*Department of Mechanical Engineering
 University of Basrah
 College of Engineering
 prosismael@yahoo.com*

Imad Abdul-Kadhem Kheioon
*Department of Mechanical Engineering
 University of Basrah
 College of Engineering
 phdimad@yahoo.com*

Abstract- An intelligent and anticipatory speed controller for internal combustion engines was designed theoretically and examined experimentally. This design was based on the addition of a torque loop to the main speed loop. The model can sense the external load with the help of a load cell and send this signal to a soft computing unit for analysis and processing. This scheme will improve the ability of anticipation of controller since it treats the factors that affect the speed, not the speed itself. The experimental design was implemented using two types of actuating techniques; an intelligent throttling actuator and an intelligent injection actuator. The signal was analyzed by using intelligent techniques such as fuzzy logic, neural network and genetic algorithm. The experimental data were used to train the neural and the Adaptive Neuro-Fuzzy Inference System. The comparison of the results obtained in this work with other available models proved the efficiency and the robustness of the present model.

KEY WORDS: Speed controller, SI Engines, Direct torque, Fuzzy logic, neural network, Genetic algorithm, ANFIS.

1. Introduction

The speed control system is a very important subject in the fields of rotary motors and engines such as electrical drives and internal combustion engines. In the internal combustion engines which represent the case study of the present work, the optimal design of speed control system is a very sensitive issue because it relates strongly with the fuel consumption and emission. In the past, speed control systems in these engines were established by using conventional and classical methods such as simple Proportional (P) controller or normal Proportional – Integral (PI) controller. By an addition of derivative action to the (PI) controller, a controller of three actions named Proportional – Integral – Derivative (PID) controller can be obtained. These controllers can be used to control the speed of simple applications but their weakness is clearly appearing in controlling complex and nonlinear systems. In order to control the systems which have uncertainty and nonlinearity, the demand for intelligent techniques is extremely appearing. These intelligent techniques such as fuzzy logic, neural network and genetic algorithm can improve the performance of speed controllers and they are very useful in the modeling of systems that do not have a certain mathematical model. Therefore, this work focuses on improving the speed controller of spark ignition engines by the use of intelligent techniques.

The speed control problem for the internal combustion engines is not a new topic in the engine control community, since regulation of the idle speed is one of fundamental control specifications for engine management.

In 1996, Anna [1] studied the control design issues for two advanced technology engines: (i) a spark ignition (SI)

engine with secondary throttles placed in the intake ports of the cylinders, and (ii) an SI engine equipped with a variable cam timing (VCT) mechanism. Both engine configurations are multivariable and nonlinear. The results demonstrated the advantages of a systematic approach to develop advanced technology power train control system.

Per Andersson [2] in 2005 presented a Ph.D. thesis which was devoted to the systematic improvement of the cylinder air charge (CAC) estimation on the turbocharged (TC) spark – ignited (SI) engines. A second objective of this work was to provide the design engineer with a flexible framework for CAC estimation that can be easily adapted to various engines. The developed model and observer were used for model – based air – fuel ratio control. A TC SI engine was controlled by the proposed controller in real time with very rapid throttle transients.

In 2005, Pushkaraj [3] studied the dynamic modeling and control of gasoline powered, four stroke, spark ignited, port fuel injection engines. In this study, an automotive engine was equipped with a control system architecture that comprised of a microcontroller, several sensors and actuators. This microcontroller can select the engine control inputs such as air flow rate, fuel flow rate, and spark timing.

In 2006, Sitthichok et al. [4] presented a research with the objective of developing a mathematical model of spark ignition engine using a cylinder-by-cylinder model approach in order to predict the performances, torque and power. Due to the nonlinear time – varying nature of the SI engine, an adaptive multi – input single – output (MISO) controller based on self – tuning regulator (STR) was proposed by Feng – Chi et al. [5] in 2007 for the idle speed control. Thomas et al. [6] in 2008 addressed the control of the airpath of a turbocharged SI engine equipped with Variable Value Timing (VVT) actuators. Also in 2008, Ahmad et al. [7] presented a control scheme which utilized the Adaptive Neuro Fuzzy Inference System (ANFIS) controller to track the rotational speed of a reference engine and disturbance rejection during engine idling. To evaluate the performance of the controller a model of the system was developed and simulation results were presented. It was shown in this study that the ANFIS controller is suitable to control the systems with large time delays.

In 2011, Osama et al. [8] investigated the effect of varying the inlet throat diameter at different degrees of Inlet Valve Close (IVC) and Inlet Valve Open (IVO) and different overlap angles on the engine performance at the design engine speed. Power, Torque, BMEP, BSFC and volumetric efficiency were calculated and presented to show the effect of varying value timing on these parameters for all the inlet throat diameters considered. In 2011, Ting et al. [9] presented a new approach for the calibration and control of

SI engines using a combination of neural networks and sliding mode control technique. From the simulation studies, the feasibility and efficiency of the proposed approach were illustrated. For both control problems of this study, excellent tracking performance has been achieved.

Mohd et al. [10] in 2011 presented the design of a PID controller for a constant speed engine. The PID controller regulated the engine speed by manipulating the throttle opening and thus determining the air–fuel intake for combustion. It comprised of a proportional (P), an integral (I), and a derivative (D) controller. The Ziegler Nicholas method was used to determine and tune the PID controller parameters. Simulation was implemented on the engine timing model with a closed loop available in Simulink – MATLAB software. The system’s output response was analyzed based on the rise time, settling time, percentage overshoot and offset.

In 2012, Aris et al. [11] introduced a method for controlling the SI engine torque using fuzzy gain scheduling. By using this method, the throttle opening commanded by the driver will be corrected by the throttle correction signal that guarantees the engine torque output will follow the desired engine torque input. In this case, a spark ignition engine with automatic transmission is used to meet a good performance under this controller design.

In 2012, the fuzzy logic engine torque regulation was used by Aris and Sumardi [12] to control the throttle position entered by the driver to achieve an optimal engine torque. From the simulation results, it can be concluded that this control strategy is very effective to reduce the fuel consumption and simultaneously to optimize the engine performance.

In 2012, Mohammad and Majid [13] designed a robust controller based on the quantitative feedback theory (QFT) on vehicles to control an engine at idle speed. This controlling approach, proposed a transparent and practical controller design methodology for uncertain single – input single – output and multivariable plants. In the engine, throttle valve dynamics has multivariable nonlinear transfer functions. For this reason, in this work, a QFT technique was used for designing the proposed controller.

2. Objectives of the Present Study

In this work, a design of speed controller system for the internal combustion engines by using intelligent techniques is presented. Also, an intelligent electronic actuator has been designed experimentally by two methods: (i) Extra intelligent injection unit and (ii) Soft computerized controlled air – fuel ratio (AFR). A Simulink model for SI engines and their speed control systems is proposed in this study as well as a new technique for estimating the rotor shaft speed without the use of a speed sensor or encoder, i.e., a sensorless (encoder-less) speed estimation.

3. Expert Systems

This hybrid technique is known as a neuro fuzzy technique. Two possible models of fuzzy neural systems are [14]:

1. In response to linguistic statements, the fuzzy interface block provides an input vector to a multi – layer neural network. The neural network can be adapted (trained) to yield desired command outputs or decisions, Fig.(1).

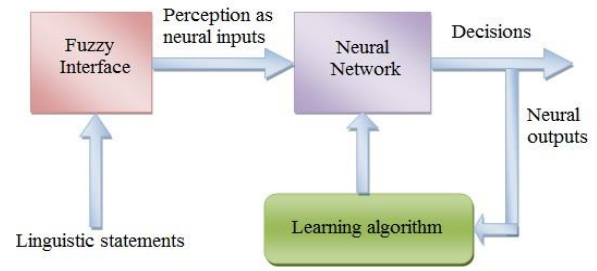


Fig.1 The first model of fuzzy neural system.

2. A multi – layered neural network drives the fuzzy inference mechanism, Fig.(2).

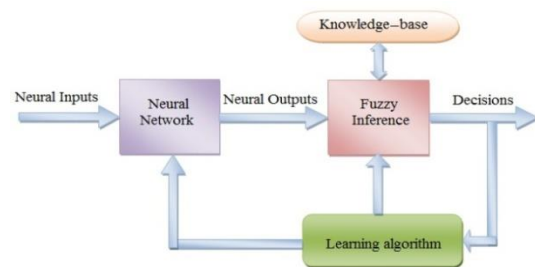


Fig.2 The second model of fuzzy neural system.

Networks are used to tune membership functions of the fuzzy systems that are employed as decision – making systems for controlling the equipment.

4. The Adaptive Network Based Fuzzy Inference System (ANFIS)

The ANFIS neurofuzzy controller was implemented by Jang (1993) and employs a Takagi – Sugeno – Kang (TSK) fuzzy inference system. The basic ANFIS architecture is shown in Fig.(3).

Square nodes in the ANFIS structure denote parameter sets of the membership functions of the TSK fuzzy system. Circular nodes are static / non – modifiable and perform operations such as product or max/min calculations. A hybrid learning rule is used to accelerate the parameter adaption. This uses sequential least squares in the forward pass to identify consequent parameters, and back – propagation in the backyard pass to establish the premise parameters.

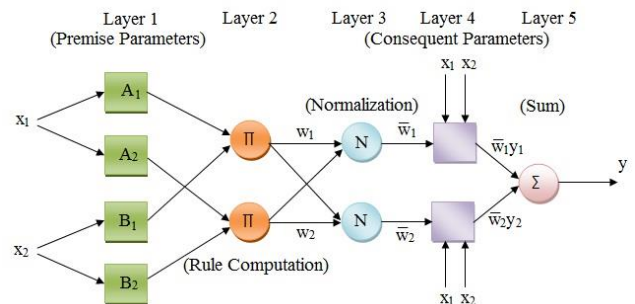


Fig.3 The Adaptive Network Based Fuzzy Inference System (ANFIS).

There are many strategies which treat the combination of fuzzy logic with neural network. In this study, the Adaptive Neuro – Fuzzy Inference System (ANFIS) will be used which was implemented by Jang (1993) and it was

functionally equivalent to Sugeno's Inference Mechanism [14]. Sugeno and Takagi use the following rules:

$$R_1: \text{if } x \text{ is } A_1 \text{ and } y \text{ is } B_1 \text{ then } z_1 = a_1x + b_1y$$

$$R_2: \text{if } x \text{ is } A_2 \text{ and } y \text{ is } B_2 \text{ then } z_2 = a_2x + b_2y \quad (1)$$

The firing levels of the rules are computed by:

$$\alpha_1 = A_1(x_0) \times B_1(y_0)$$

$$\alpha_2 = A_2(x_0) \times B_2(y_0) \quad (2)$$

Where the logical AND can be modeled by any continuous t-norm, e.g.,

$$\alpha_1 = A_1(x_0) \wedge B_1(y_0)$$

$$\alpha_2 = A_2(x_0) \wedge B_2(y_0) \quad (3)$$

Then the individual rule outputs are derived from the relationships:

$$z_1 = a_1 x_0 + b_1 y_0$$

$$z_2 = a_2 x_0 + b_2 y_0 \quad (4)$$

And the crisp control action is expressed as:

$$z_0 = \frac{\alpha_1 z_1 + \alpha_2 z_2}{\alpha_1 + \alpha_2} = \beta_1 z_1 + \beta_2 z_2 \quad (5)$$

Where β_1 and β_2 are the normalized values of α_1 and α_2 with respect to the sum $(\alpha_1 + \alpha_2)$, i.e.:

$$\beta_1 = \frac{\alpha_1}{\alpha_1 + \alpha_2}$$

$$\beta_2 = \frac{\alpha_2}{\alpha_1 + \alpha_2} \quad (6)$$

For simplicity, only two rules and two linguistic values have been assumed for each input variable. The layers of (ANFIS) can be described as follows:

A. Layer (1) :The output of the node is the degree to which the given input satisfies the linguistic label associated to this node. Usually, bell-shaped membership functions are chosen to represent the linguistic terms as shown in the following equation :

$$A_i(u) = \exp \left[-\frac{1}{2} \left(\frac{u - a_{i1}}{b_{i1}} \right)^2 \right]$$

$$B_i(v) = \exp \left[-\frac{1}{2} \left(\frac{v - a_{i2}}{b_{i2}} \right)^2 \right] \quad (7)$$

Where $\{a_{i1}, a_{i2}, b_{i1}, b_{i2}\}$ is the parameter set. As the values of these parameters change, the bell-shaped functions vary accordingly, thus exhibiting various forms of membership functions on the linguistic labels A_i and B_i . In fact, any continuous function, such as trapezoidal and triangular-shaped membership functions, are also quantified candidates for node functions in this layer. Parameters in this layer are referred to as premise parameters.

B. Layer (2): Each node computes the firing strength of the associated rule. The output of top neuron is:

$$\alpha_1 = A_1(x_0) \times B_1(y_0) = A_1(x_0) \wedge B_1(y_0) \quad (8)$$

And the output of the bottom neuron is:

$$\alpha_2 = A_2(x_0) \times B_2(y_0) = A_2(x_0) \wedge B_2(y_0) \quad (9)$$

Both nodes in this layer are labeled by T, because other t-norms can be chosen for modeling the logical AND operator. The nodes of this layer are called rule nodes.

C. Layer (3) : Every node in this layer is labeled by (N) to indicate the normalization of the firing levels. The output of top neuron is the normalized (with respect to the sum of firing levels) firing level of the first rule:

$$\lambda_1 = \frac{\alpha_1}{\alpha_1 + \alpha_2} \quad (10)$$

And the output of the bottom neuron is the normalized firing level of the second rule :

$$\lambda_2 = \frac{\alpha_2}{\alpha_1 + \alpha_2} \quad (11)$$

D. Layer (4): The output of top neuron is the product of the normalized firing level and the individual rule output of the first rule:

$$\lambda_1 z_1 = \lambda_1(a_1 x_0 + b_1 y_0) \quad (12)$$

the output of the bottom neuron is the product of the normalized firing level and the individual rule output of the second rule :

$$\lambda_2 z_2 = \lambda_2(a_2 x_0 + b_2 y_0) \quad (13)$$

E. Layer (5) :The single node in this layer computes the overall system output as the sum of all incoming signals, i.e.,

$$z_0 = \lambda_1 z_1 + \lambda_2 z_2 \quad (14)$$

If a crisp training set $\{(x^k, y^k), k = 1, \dots, K\}$ is given, then the parameters of the hybrid neural net (which determine the shape of the membership functions of the premises) can be learned by descent-type methods. This architecture and learning procedure is called ANFIS (adaptive-network-based fuzzy inference system) by Jang [14].

The error function for pattern k can be given by:

$$E_k = (y^k - O^k)^2 \quad (15)$$

Where y^k is the desired output and O^k is the computed output by the hybrid neural net.

5. Modeling of SI Engine and its Intelligent Speed Control system

5.1 Intake Manifold

Assuming isothermal conditions, the intake manifold pressure dynamics can be modeled as:

$$\frac{d}{dt} p_m = \frac{R T_m}{V_m} (\dot{m}_{ai} - \dot{m}_{ao}) \quad (16)$$

Where p_m , T_m , and V_m are the manifold pressure, temperature and volume respectively, and \dot{m}_{ai} is the air mass flow rate through the throttle. The air mass flow rate exiting the intake manifold and entering the engine is denoted in the above equation by \dot{m}_{ao} . The air gas constant, R , is equal to (287 J/kg.k). The schematic representation of SI engine is shown in the Fig.(4).

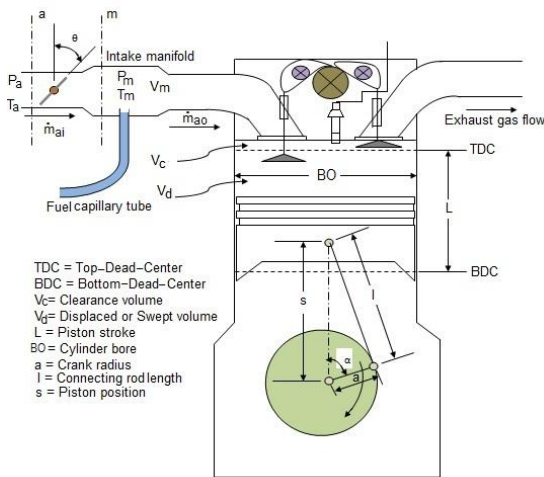


Fig.4 Schematic of gasoline engine with piston and cylinder geometry.

The air mass flow rate , \dot{m}_{ai} , will be derived in this section. The continuity equation between the positions (a) and (m) in Fig.(4) can be written as:

$$\dot{m}_{ai} = \rho_a A_a u_a = \rho_m A_m u_m \quad (17)$$

Where ρ_a and u_a are the density and velocity of air at the section (a) respectively, while ρ_m and u_m are the same previous parameters at the section (m). the areas at sections (a) and (m) are named as A_a and A_m respectively. The cross-sectional area at throttling position may be approximated as :

$$A(\theta) = \frac{\pi}{4} d^2 (1 - \cos^2(\theta)) \quad (18)$$

Equation (17) can be rewritten for u_a as follows:

$$u_a = u_m \frac{A_m \rho_m}{A_a \rho_a} \quad (19)$$

The steady state energy equation between sections (a) and (m) can be defined as:

$$g z_a + \frac{u_a^2}{2} + p_a V_a + E_a + Q = g z_m + \frac{u_m^2}{2} + p_m V_m + E_m + W \quad (20)$$

The terms $(g z_a)$ and $(g z_m)$ may be neglected when taking a horizontal flow condition. Also, at the case of no heat transfer, Q , and no external work, W , done on the system ,the terms Q and W can be cancelled from the last equation. The flow energy (PV) and internal energy (E) can be expressed in terms of the enthalpy (h) as follows:

$$\begin{aligned} h_a &= p_a V_a + E_a \\ h_m &= p_m V_m + E_m \end{aligned} \quad (21)$$

Substituting equation (21) in equation (20) yields :

$$\frac{u_m^2 - u_a^2}{2} = (h_a - h_m) \quad (22)$$

Then, Substituting equation (19) in equation(22) gives :

$$u_m = \sqrt{\frac{2(h_a - h_m)}{1 - \left(\frac{A_m \rho_m}{A_a \rho_a}\right)^2}} \quad (23)$$

Substituting equation (23) in equation (17) yields:

$$\dot{m}_{ai} = \rho_m A_m u_m = \rho_m A_m \sqrt{\frac{2(h_a - h_m)}{1 - \left(\frac{A_m \rho_m}{A_a \rho_a}\right)^2}} \quad (24)$$

With the relation $(h = c_p T)$, where c_p is the specific heat of air at constant pressure, the last equation can be written as:

$$\dot{m}_{ai} = \frac{A_m \rho_m}{\sqrt{1 - \left(\frac{A_m \rho_m}{A_a \rho_a}\right)^2}} \times \sqrt{2} \times \sqrt{c_p (T_a - T_m)}$$

Which can be rearranged as:

$$\dot{m}_{ai} = \frac{A_m \rho_m}{\sqrt{1 - \left(\frac{A_m \rho_m}{A_a \rho_a}\right)^2}} \times \sqrt{2} \times \sqrt{c_p T_a \left(1 - \frac{T_m}{T_a}\right)} \quad (25)$$

The flow is isentropic(reversible adiabatic) ,so the following relations may be considered:

$$p_a V_a^\gamma = p_m V_m^\gamma \quad (26)$$

Where γ is the ratio of the specific heats $\left(\frac{c_p}{c_v}\right)$. In another

form, the above equation becomes:

$$\frac{p_a}{p_m} = \left(\frac{V_m}{V_a}\right)^\gamma \quad (27)$$

Also, the gas constant, R , is written as :

$$\frac{p_a v_a}{T_a} = \frac{p_m v_m}{T_m} = R \quad (28)$$

Rearranging the last equation results in:

$$\frac{T_m}{T_a} = \frac{p_m v_m}{p_a v_a} \quad (29)$$

Substituting equation (27) in the equation (29) yields:

$$\frac{T_m}{T_a} = \frac{p_m}{p_a} \left(\frac{p_a}{p_m}\right)^{\frac{1}{\gamma}} = \left(\frac{p_m}{p_a}\right)^{\frac{\gamma-1}{\gamma}} \quad (30)$$

Now, substituting this last equation in the equation (25) gives:

$$\begin{aligned} & \frac{A_m \rho_m}{\sqrt{1 - \left(\frac{A_m \rho_m}{A_a \rho_a}\right)^2}} \times \\ & \sqrt{2} \times \\ & \sqrt{c_p T_a \left(1 - \left(\frac{p_m}{p_a}\right)^{\frac{\gamma-1}{\gamma}}\right)} \\ & \dot{m}_{ai} = \end{aligned} \quad (31)$$

Noting that

$$c_p = \frac{\gamma}{\gamma-1} R$$

Then :

$$\dot{m}_{ai} = \frac{A_m \rho_m}{\sqrt{1 - \left(\frac{A_m \rho_m}{A_a \rho_a}\right)^2}} \times \sqrt{2} \times \sqrt{\frac{\gamma}{\gamma-1} R T_a \left(1 - \left(\frac{p_m}{p_a}\right)^{\frac{\gamma-1}{\gamma}}\right)} \quad (32)$$

The term $\sqrt{1 - \left(\frac{A_m \rho_m}{A_a \rho_a}\right)^2}$ is approximately equal to

(1).Thus, by multiplying and dividing the right side of equation (32) by the term $\sqrt{R T_a}$,it becomes:

$$\dot{m}_{ai} = \frac{A_m \rho_m R T_a}{\sqrt{R T_a}} \times \sqrt{2 \left(\frac{\gamma}{\gamma-1}\right) \left(1 - \left(\frac{p_m}{p_a}\right)^{\frac{\gamma-1}{\gamma}}\right)} \quad (33)$$

From the ideal gas properties, it is well-known that:

$$R T_a = p_a V_a = \frac{p_a}{\rho_a} \quad (34)$$

Substituting equation (34) in the equation (33) yields:

$$\dot{m}_{ai} = \frac{A_m \rho_m \frac{p_a}{\rho_a}}{\sqrt{R T_a}} \times \sqrt{2 \left(\frac{\gamma}{\gamma-1}\right) \left(1 - \left(\frac{p_m}{p_a}\right)^{\frac{\gamma-1}{\gamma}}\right)} \quad (35)$$

Knowing that:

$$\frac{\rho_m}{\rho_a} = \left(\frac{p_m}{p_a}\right)^{\frac{1}{\gamma}}$$

Then, it can be found that:

$$\dot{m}_{ai} = \frac{A_m p_a}{\sqrt{R T_a}} \left(\frac{p_m}{p_a}\right)^{\frac{1}{\gamma}} \times \sqrt{2 \left(\frac{\gamma}{\gamma-1}\right) \left(1 - \left(\frac{p_m}{p_a}\right)^{\frac{\gamma-1}{\gamma}}\right)} \quad (36)$$

Finally, for real flow, the discharge coefficient, c_d , for the flow should be taken into account. Then, the air mass flow rate is given by:

$$\dot{m}_{ai} = \frac{c_d A_m p_a}{\sqrt{R T_a}} \left(\frac{p_m}{p_a}\right)^{\frac{1}{\gamma}} \times \sqrt{2 \left(\frac{\gamma}{\gamma-1}\right) \left(1 - \left(\frac{p_m}{p_a}\right)^{\frac{\gamma-1}{\gamma}}\right)} \quad (36)$$

Equation (36) is used for the compressible flow and depending on the pressure ratio, p_r , which equal to $\left(\frac{p_m}{p_a}\right)$,

this equation can be rearranged in the following expression, as it was given by [15]:

$$\dot{m}_{ai} = c_d A_m \frac{p_a}{\sqrt{R T_a}} \psi \left(\frac{p_m}{p_a}\right) \quad (37)$$

Where the flow function, $\psi \left(\frac{p_m}{p_a}\right)$, is defined by [15].

Where p_{rc} is the critical pressure ratio and it is calculated from the relation:

$$p_{rc} = \left(\frac{2}{\gamma+1}\right)^{\frac{\gamma}{\gamma-1}} \quad (38)$$

For incompressible flow, the air mass flow rate can be derived starting from equation (36). The last term which has the pressure ratio in this equation can be rewritten as:

$$\left(\frac{p_m}{p_a}\right)^{\frac{\gamma-1}{\gamma}} = \left(1 - \frac{p_a - p_m}{p_a}\right)^{\frac{\gamma-1}{\gamma}} = \left(1 - \frac{\Delta p}{p_a}\right)^{\frac{\gamma-1}{\gamma}} \quad (39)$$

Where,

$$\Delta p = p_a - p_m$$

Using the binomial theorem, equation (39) can be written as:

$$\left(\frac{p_m}{p_a}\right)^{\frac{\gamma-1}{\gamma}} = 1 - \frac{\gamma-1}{\gamma} \frac{\Delta p}{p_a} - \left[\frac{\gamma-1}{\gamma} \left(\frac{\gamma-1}{\gamma} - 1\right) \frac{1}{2} \left(\frac{\Delta p}{p_a}\right)^2\right]$$

Which may be reduced to:

$$\left(\frac{p_m}{p_a}\right)^{\frac{\gamma-1}{\gamma}} \cong 1 - \frac{\gamma-1}{\gamma} \frac{\Delta p}{p_a} \quad (40)$$

Substituting equation(40) in equation (35) provides:

$$\begin{aligned} \dot{m}_{ai} &= \frac{c_d A_m p_a}{\sqrt{R T_a}} \left(\frac{p_m}{p_a}\right)^{\frac{1}{\gamma}} \times \sqrt{2 \left(\frac{\gamma}{\gamma-1}\right) \left(1 - 1 + \left(\frac{\gamma-1}{\gamma}\right) \frac{\Delta p}{p_a}\right)} \\ &= \frac{c_d A_m p_a}{\sqrt{R T_a}} \left(\frac{p_m}{p_a}\right)^{\frac{1}{\gamma}} \times \sqrt{2 \frac{\Delta p}{p_a}} \end{aligned}$$

$$= \frac{c_d A_m \sqrt{p_a}}{\sqrt{R T_a}} \left(\frac{p_m}{p_a}\right)^{\frac{1}{\gamma}} \times \sqrt{2 \Delta p}$$

Simplifying the last equation by putting $\sqrt{\frac{p_a}{R T_a}} = \sqrt{\rho_a}$,

and then using the relation :

$$\left(\frac{p_m}{p_a}\right)^{\frac{1}{\gamma}} = \frac{\rho_m}{\rho_a}$$

Gives:

$$\dot{m}_{ai} = c_d A_m \rho_m \sqrt{\frac{2(p_a - p_m)}{\rho_a}} \quad (41)$$

For an incompressible flow, it is clearly noted that $\rho_a = \rho_m$. Hence, the last equation can be simplified to :

$$\dot{m}_{ai} = c_d A_m \sqrt{2 \rho_a (p_a - p_m)} \quad (42)$$

The air mass flow rate can be found experimentally as in the following formula, which was presented by Fathi and Ammar [16] in 1996:

$$\dot{m}_{ai} = (1 + 0.907 \theta + 0.0998 \theta^2) g(p) \quad (43)$$

Where θ is the the throttling angle and $g(p)$ is the pressure function, which was given by:

$$g(p) = 0.0197 \sqrt{101.325 p - p^2}$$

$$p \geq 50.6625$$

The air mass flow rate entering the engine can be expressed as:

$$\dot{m}_{ao} = \frac{V_d \eta_v \omega p_m}{4 \pi R T_m} \quad (44)$$

Where V_d is the displaced cylinder volume, ω , is the engine speed in rad/sec, and η_v is the volumetric efficiency. The displaced volume can be obtained as:

$$V_d = \frac{\pi}{4} B O^2 L \quad (45)$$

Where BO is the cylinder bore and L is the piston stroke as shown in the Fig.(4). Equation (44) was given by many references with different forms such as Zhang et al.[17] in 2008 and Thomas et al.[18] in 2009. An experimental formula was given by DaeEun and Jaehong [19] in 2007 in order to calculate (\dot{m}_{ao}) by formulating it as a function of the manifold pressure and engine speed as shown in the equation:

$$\dot{m}_{ao} = - 0.0005968 N - 0.1336p + 0.0005341 Np + 0.000001757 Np^2 \quad (46)$$

Where N is the engine speed in (RPM). In some SI engine models, the air mass flow rate exiting the manifold and entering the engine may be expressed as[15]:

$$\dot{m}_{ao} = \frac{m_{mix}}{1 + AF_s / \phi} \quad (47)$$

Where AF_s is the stoichiometric Air-Fuel ratio and ϕ is the equivalence ratio which is defined as:

$$\phi = \frac{(FA)_{act}}{(FA)_{stoich}} = \frac{(AF)_{stoich}}{(AF)_{act}} \quad (48)$$

Thailand, 18 – 20 October 2006, Nakhon Ratchasima, Thailand, 2006.

[5] Feng – Chi Hsieh, Bo – Chiu Chen and Yuh – Yih Wu, “Adaptive Idle Speed Control for Spark– Ignition Engines”, SAE International, 2007 – 01 – 1197, 2007.

[6] Thomas Leroy, Jonathan Chauvin and Nicolas Petit, “Airpath Control of a SI Engine with Variable Valve Timing Actuators”, 2008 American Control Conference, USA, 2008.

[7] Ahmad Reza Mohtadi, Hamed Torabi and Mohammad Osmani, “Design of Neuro–Fuzzy Controller For Idle speed Control”, 9th WSEAS International Conference on Neural Networks, Sofia, Bulgaria, May 2 – 4, 2008.

[8] Osama H. Ghazal, Yousef S. Najjar and Kutaeba J. AL – Khishali, “Effect of Varying Inlet Valve Throat Diameter at Different IVO, IVC, and Overlap Angles on SI Engine Performance” , Proceedings of the World Congress on Engineering 2011 Vol. III, WCE 2011, July 6 – 8, 2011, London, U.K, 2011.

[9] Ting Huang, Hossein Javaherian and Derong Liu, “Nonlinear Torque and Air – To – Fuel Ratio Control of Spark Ignition Engines Using Neuro – Sliding Mode Techniques”, International Journal of Neural Systems, Vol. 21, No.3, PP. 213 – 224, 2011.

[10] Mohd Khair H, Aishwarya K., Ribhan Zafira A. R. and Siti Anom A. , “Design a PID Controller for a Constant Speed of Combustion Engine”, Australian Journal of Basic and Applied Sciences, 5(12) : 1586 – 1593, 2011.

[11] Aris Triwiyatno, Mohammad Nuh, Ari Santoso and I Nyoman Sutantra, “Engine Torque Control System Using Fuzzy Gain Scheduling for Spark Ignition Engine Application”, IJEERI, Vol. 1, No.1, 2012.

[12] Aris Triwiyatno and Sumardi, “Fuel Saving Strategy in Spark Ignition Engine Using Fuzzy Logic Engine Torque Control”, MAKARA, TEKNOLOGI, Vol.16, No.1, PP. 35 – 42, 2012.

[13] Mohammad Reza Gharib and Majid Moavenian, “A New Generalized Controller for Engine in Idle Speed Condition”, J. Basic Appl. Sci. Res., 2(7) , 6596 – 6604, 2012.

[14] Robert Fuller, “Neural Fuzzy Systems”, Abo Akademi University , ISBN951 – 650 – 624 – 0, ISSN 0358 – 5654, 1995.

[15] Lino Guzzella and Christopher H. Onder , “ Introduction to Modeling and Control of Internal Combustion Engine Systems”, Springer, 2010.

[16] Fathi M. Salam and Ammar B. Gharbi, “ Temporal Neuro–Control of Idle Engine Speed ” ,Proc. of International symposium on Intelligent Control, Dearborn, Michigan, pp.396–401 ,1996.

[17] J. Zhang , T. Shen and R. Marino, “ Model–Based Cold–Start Speed Control Design for SI Engines ”, Proceedings of the 17th World Congress, The International Federation of Automatic Control, seoul, Korea ,July 6–11 ,pp.1042–1047 ,2008.

[18] Thomas Leroy ,Jonathan Chauvin and Nicolas Petit , “ Motion Planning for Experimental Air Path Control of a Variable–Valve–Timing Spark Ignition Engine”, Control Engineering Practice 17,pp.1432–1439, 2009.

[19] DaeEun Kim and Jaehong Park , “ Application of Adaptive Control to the Fluctuation of Engine Speed at Idle ”, Information Sciences 177, pp.3341–3355, 2007.

[20] Willard W. Pulkrabek , “ Engineering Fundamentals of the Internal Combustion Engine”, Prentice Hall, 1990.

[21] John B. Heywood , “ Internal Combustion Engine Fundamentals ”, McGraw–Hill, Inc., 1988.

[22] Nader Barsoum, “Performance of Direct Torque Control Implemented in Speed Drive”, Global Journal of Technology & Optimization, Vol. 3, 2012.

[23] Chandra Sekhar O. and Chandra Sekhar K., “Space Vector Modulation & Fuzzy PID Speed Controller for Direct Torque Control Induction Motor Drive”, Journal of Theoretical and Applied Information Technology, Vol. 35, No.1, PP. 126 – 134, 2012.

[24] John. J. Paserba, Masaru Shimomura, Seiichi Tanaka, Donald J. Shoup and Robert T. Hellested, “Enhanced Generator Controls for the Improving of Power System Voltage Stability”, Symposium of Specialists in Electric Operational and Expansion Planning (VIII SEPOPE) Brasilia, Brazil, May 19 – 23,2002.

[25] Johan Olsson , “Automatic Tuning of Control Parameters for Single Speed Engines”, M. Sc. Thesis, Royal Institute of Technology,2004.

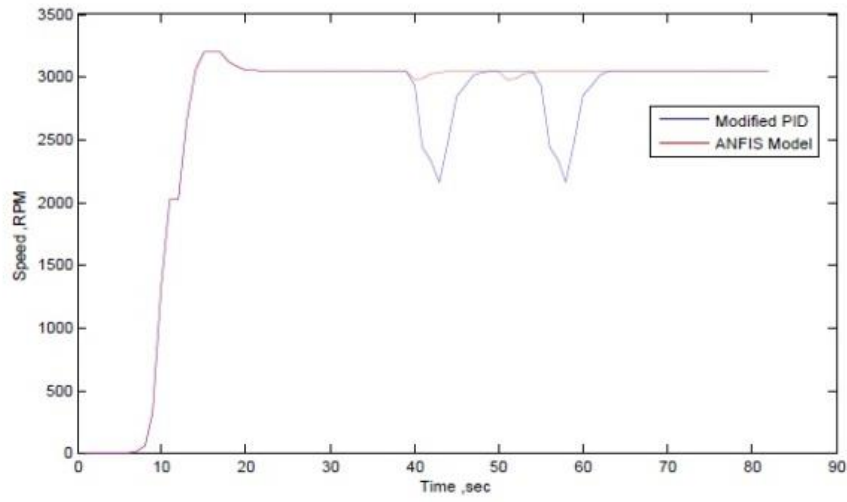


Fig.7 Comparison between ANFIS and Modified PID controller.

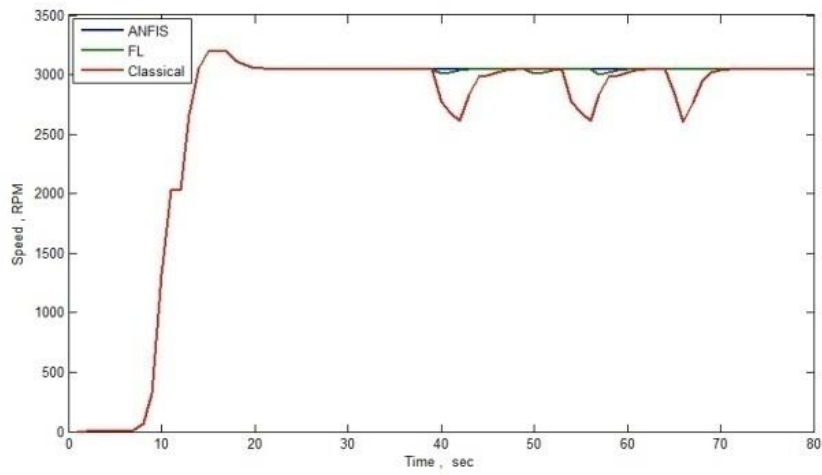


Fig.8 Comparison at three excessive loads of magnitude (400W).

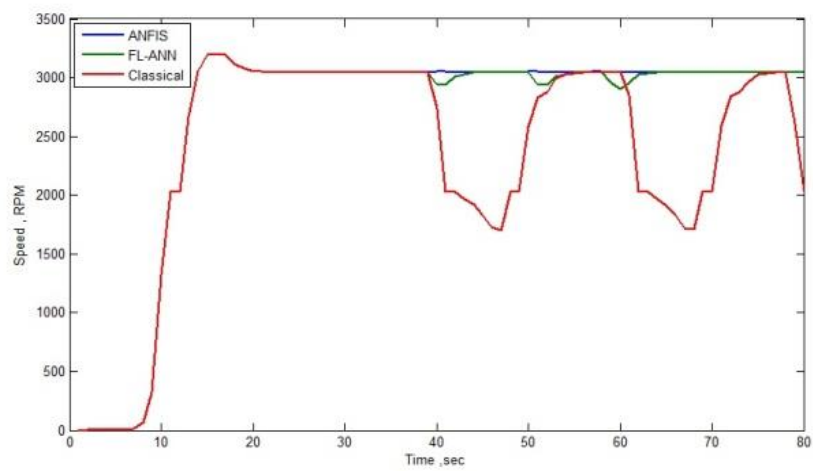


Fig.9 Comparison at three excessive loads of magnitude (500W).

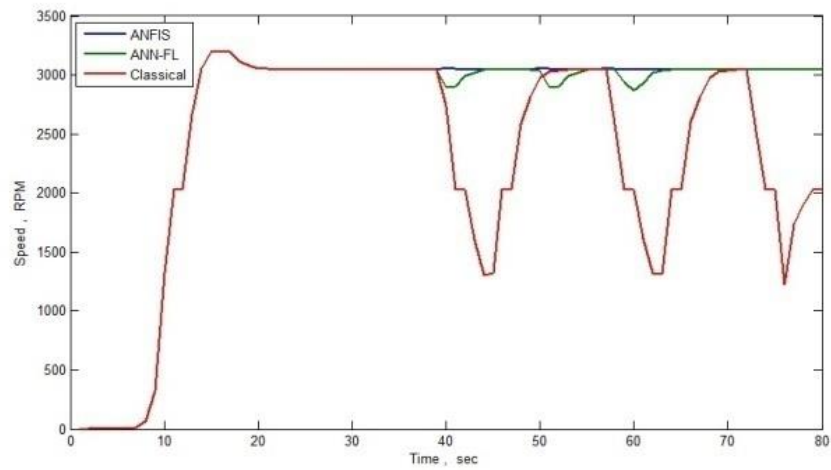


Fig.10 Comparison at three excessive loads of magnitude (600W).

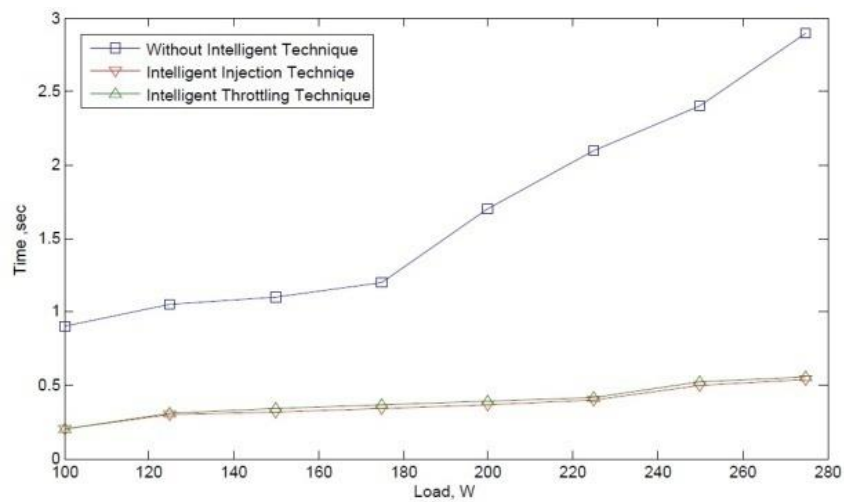


Fig.11 Testing of the two proposed experimental techniques.

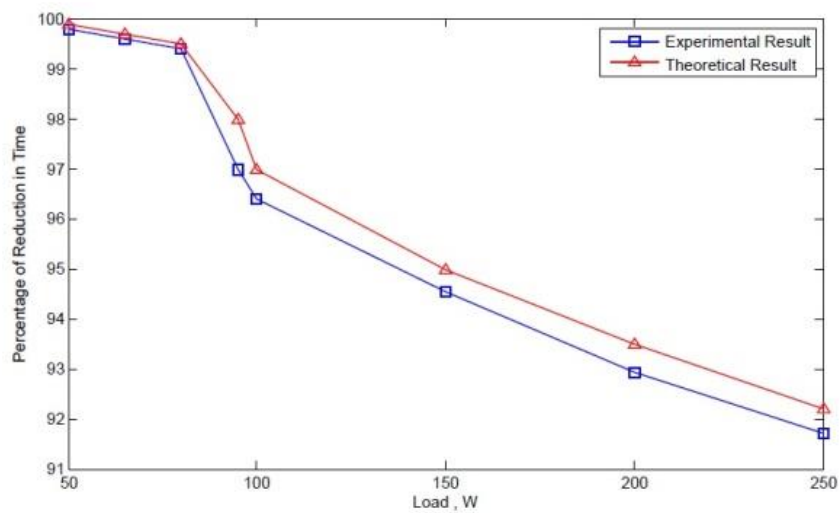


Fig.12 Comparison between theoretical and experimental results.